Egypt. J. Rad. Sci. Applic. **Vol. 36,** No. 1-2, pp.33 - 45 (2023)

Egyptian Journal of Radiation Sciences and Applications
http://ejrsa.journals.ekb.eg/

EGYPTIAN ATOMIC ENERGY AUTHORITY

Saccharomyces cerevisiae - Fermented Garlic Attenuates Gamma-Irradiation Induced Brain and Liver Toxicity via Regulation of the NF-κB and STAT3 Signaling Pathway

Sawsan M. El-Sonbaty[(1)], Hanan A. Fahmy[(2)], Amel F. M. Ismail[(2)#]

[(1)]Radiation Microbiology Department, National Center for Radiation Research and Technology (NCRRT), Egyptian Atomic Energy Authority, Cairo, Egypt; [(2)]Drug Radiation Research Department, National Center for Radiation Research and Technology (NCRRT), Egyptian Atomic Energy Authority, Cairo, Egypt.

THE PRESENT study was designed to evaluate the radio-protective effects of *Saccharomyces cerevisiae*-fermented garlic extract (FGE) on γ-irradiation-induced acute toxicity in rats' brain and liver. The rats were divided into four groups, Group I (C; control group), Group II (FGE), III (R: irradiated rats), Group IV (FGE+R). In C, and R groups rats were administered orally with 1 ml of water, and in FGE, and FGE+R groups, rats administered orally with 1 ml of FGE. At day 21, R and FGE+R groups were exposed to a single shot of whole-body gamma irradiation (6 Gy). The results showed that γ-irradiation significantly increased the activity of the hepatic enzymes; ALT, AST, ALP, GGT, and the levels of total-cholesterol (TC), and triglycerides (TG) in the serum. In addition, the activity of SOD, and GSH-Px were significantly decreased, with alteration in the trace elements levels were observed in the brain and liver cytosolic fractions. Moreover, the levels of MDA, and the pro-inflammatory markers; TNF-α, IL-1β, IL-6 and caspase-3 activity were significantly elevated, GSH content was significantly decreased ($P<0.001$), the gene expression ratios of NF-κB and STAT3 showed significant up-regulation ($P<0.001$), as well as, DNA fragmentations were observed in brain and liver tissues. FGE pre-treatment has significantly ameliorated the changes in all these studied parameters. The histopathological investigations confirmed these biochemical changes in the brain and liver tissues. These findings could suggest that the bioactivities of FGE showed neuro-hepato-protective effects on acute toxicity of gamma irradiation, by improving the antioxidant, anti-inflammatory and anti-apoptotic activities associated with regulation of the NF-κB and STAT3 signaling pathway in rats' brain and liver.

Keywords: Antioxidant status, Fermentation, Radioprotection, Trace elements, Yeast.

Introduction

Ionizing radiation (IR) is widely used in several fields. In medical applications, IR is a useful tool for treatment and diagnosis of various diseases (Ansari et al., 2021). The beneficial impact of IR is accompanied by detrimental consequences that hinder the radiotherapy process (Ibrahim et al., 2023; Owis et al., 2023). The interaction between IR and tissues stimulates various radiobiological impairments in the normal tissues. IR promotes lipid per-oxidation (LPO) in tissues and cells, which is proportional to the dose of gamma-irradiation. In addition, IR promotes water radiolysis, and the release of reactive oxygen species (ROS) (Rageh & El-Gebaly, 2018; Ozmen & Kavrik, 2020; Ansari et al., 2021). Living cells possess endogenous antioxidant enzymatic and non-enzymatic mechanisms to maintain the redox equilibrium. However, when the ROS exceeds the cellular antioxidant capability, it triggers cellular oxidative stress, inflammation, and destruction of cellular organelles, such as DNA, RNA, proteins, and membranes, causing

[#]Corresponding Author: Email: afmismail@gmail.com
Received 19/09/2023; Accepted 4/10/2023
DOI: 10.21608/EJRSA.2023.236135.1161

cellular dysfunction and mortality (Wei et al., 2019; Ansari et al., 2021; Ibrahim et al., 2023; Hussien, 2023). Oxidative stress is involved in the development of pathological conditions, such as hepatotoxicity and neurotoxicity. Brain and liver are sensitive organs that are strongly affected by oxidative damage. Radiotherapy is used to treat head and neck cancers. The normal tissues of the brain are influenced by radiation, which caused the decay of the cognitive function, memory, and behavioral activity, accompanied by several neural complications that can persist for a long period of time and affect the patients' life (Wang et al., 2019; Abd El-Haleem et al., 2022). The central nervous system is affected by radiation, causing functional changes in neurons, and hippocampal lesions. Hippocampus impairment instigates memory problems, and is associated with various syndromes, such as Alzheimer's and schizophrenia. In addition, neuronal damage in the hippocampus can lead to hippocampal sclerosis and epilepsy (Uzun et al., 2023). The brain is subjected to oxidative damage risk due to its abundant unsaturated fatty acids, oxidizable substrates, and trace elements, as well as, relatively inadequate antioxidant enzymes (Liu et al., 2007; Uzun et al., 2023). Exposure to IR enhances LPO and free radicals release in neuronal cells. Neuron membranes in brain tissue are simulated by free radicals that originate further lipid per-oxidation. Augmented oxidative stress affects the structure and function of neurons, which assists in the development of neurological diseases. The pathogenesis of radiation-induced brain injury comprises oxidative stress, immune-inflammatory response, and vascular and blood-brain barrier (BBB) damage (Uzun et al., 2023). The liver is a highly metabolically active organ that plays an essential role in metabolism and detoxification (Akbarzadeh et al., 2015). Exposure to radiation causes hepatotoxicity in normal cells and may be associated with severe damage to hepatic tissue, which restricts the radiotherapy process, and threatens life (Zaher et al., 2016; Eassawy et al., 2020). Therefore, protection against IR-induced brain and liver damage is necessary.

Nuclear factor kappa B (NF-κB) is a pivotal transcription factor. Activation of NF-κB mediates inflammation as well as the progress of various diseases including different malignant tumors (Mohan et al., 2022). Gamma-irradiation exposure leads to the release of pro-inflammatory cytokines as tumor necrosis factor-alpha (TNF-α), interleukin-1beta (IL-1β), and interleukin-6 (IL-6) which motivates NF-κB activation (Han et al., 2006; Lestaevel et al., 2008; Ismail et al., 2016a, b; Eassawy et al., 2021). IL-6 and NF-κB are in a cooperative relation and activate each other. IL-6 activated by NF-κB stimulates the phosphorylation activation of the Signal transducer and activator of transcription (STAT3). Moreover, IL-1β, which stimulates NF-κB p65 promotes STAT3 phosphorylation. On the other hand, STAT3 activation causes the expression of various genes involved in normal cell growth, while during stress, STAT3 activation induces apoptosis (Heinrich et al., 2003; Yoshida et al., 2004; Yuan et al., 2004; Grivennikov & Karin, 2010; Mohan et al., 2022).

Ionizing radiation is a well-known cytotoxic and mutagenic agent that causes a variety of changes depending on exposed and absorbed doses, duration of exposure, interval after exposure, and susceptibility of tissues. The injury of IR to living cells is mainly due to the oxidative stress. Interactions of IR with deoxy-ribonucleic acid (DNA) involve the ionization of DNA and its reaction with surrounding water molecules, followed by decomposition of the molecular structure of DNA by the induced radicals. IR may cause damage to both the DNA and protein, due to the attack by $^{\bullet}OH$ radicals produced by water radiolysis and thus affect their ability to form complex (Wallace, 1998; Ward, 1999). Several studies dealing with radiation damage to DNA-protein complexes have reported a radiation-induced destabilization of the complexes mainly due to the protein damage (Ward, 1999). IR induces predominantly single-strand breaks, double-strand breaks, alkali labile sites, and oxidized purines and pyrimidines (Frankenberg-Schwager & Frankenberg, 1990; Halliwell & Aruoma, 1991). Numerous molecules participate in the response to radiation stress which provokes cell-damage, and cell death including caspases. Apoptosis is a complicated mechanism activated post radiation exposure (Santos et al., 2017). Caspases involved in the apoptosis as initiator (caspase-8 and caspase-9) or executioner (caspase-3, caspase-6, and caspase-7) (Sahoo et al., 2023). Caspase-3 is activated and involved in apoptosis and DNA fragmentation post exposure to IR (Santos et al., 2017).

Garlic (*Allium sativum*) has been extensively studied for its potential health benefits, and has

been used for culinary and medicinal purposes since ancient times. Garlic is recognized as medicinal functional food that is highly produced and consumed in South Asia, USA and Egypt (Lee et al., 2020; Rouf et al., 2020; Ding et al., 2023). Garlic is rich in bioactive organo-sulfur and organo-selenium compounds, such as allicin, allixin, alliin, and allylsulfides, such as diallyl disulfide (DADS), diallyl trisulfide (DATS), vinyldithiin, S-allyl mercapto cysteine (SAMC), and S-allyl-L-cysteine (SAC), in addition to amino acids, minerals and vitamins (Kim et al., 2012). These compounds contribute to the distinct flavor and aroma of garlic and are responsible for the physiological properties of garlic, such as antioxidant, anti-inflammatory, antimicrobial, immune-modulatory, anti-hyperlipidemic, anti-hypertensive, anticancer, neuro-protective, and hepato-protective activities (El-Saber Batiha et al., 2020; Herrera-Calderon et al., 2021; Mondal et al., 2022; Ding et al., 2023). The molecular mechanisms of garlic biological activities may include protective actions through its ability to scavenge ROS, such as $^{\bullet}O_2$ and H_2O_2, which cause cellular dysfunction and subsequent cell death (Ide & Lau, 2001). Allicin (diallylthiosulfinate) is the most potent organosulfur compound in garlic that is formed from alliin (S-allyl cysteine sulfoxide) in a conversion reaction catalyzed by alliinase enzyme. Allicin is a lipophilic low molecular weight molecule with high permeability that allows it to pass through the phospholipid bilayers and the BBB. Hydrogen sulfide (H_2S) is released after ingestion of allicin. The released H_2S is responsible for several biological activities, including, the anti-inflammatory efficacy, by hindering the release of pro-inflammatory cytokines thus preserving tissues from damage. In addition, H_2S acts as a neuro-modulator, diminish the neural oxidative stress, support neuronal survival, and boost the cognitive function, thus, prevents the neurodegenerative diseases, such as Alzheimer (Savairam et al., 2023). The antioxidant activity of garlic could be potentiated by different processing methods, such as aging and fermentation to increase the bioactivity of garlic (Lee et al., 2009; Queiroz et al., 2009). Aging black garlic is a modified garlic, produced by aging processes of whole garlic at high temperatures and humidity, which enrich the water soluble constituents and the polyphenol content with outcome of enhancement of its scavenging activity (Jeong et al., 2016; Chae et al., 2023). Fermentation of garlic with yeast is another method to increase the bioactivity of garlic. The fermentation process plays an active role in the physical, nutritional, and organo-leptic modifications of the starting material (Ao et al., 2011; Jung et al., 2011; Kim et al., 2012). Fermentation is one of the oldest forms of food processes in the world (Díaz-Muñoz et al., 2022). Plentiful microorganisms, including yeasts involved in the fermentation processes, as a consequence, are liable for converting sugars into alcohols along with secondary metabolites, which have an effect on the fermented beverages taste. The modern yeast biotechnology outcomes form the backbone of many commercially important sectors, including foods, beverages, pharmaceuticals, industrial enzymes and etc. *Saccharomyces cerevisiae* (*S. cerevisiae*) or baker's yeast is the foremost yeast species utilized in brewing and responsible for the various fermented beverages manufacture (Varela et al., 2023). As a consequence, *S. cerevisiae* has shown various technological properties, in addition to the fact that it is the only yeast produced and consumed as a pharmaceutical and medical product offering numerous valuable effects; for instance prevention and treatment of intestinal diseases, ameliorating abdominal pain in the irritable bowel syndrome, as well as, developing immune-modulating effects (Moslehi-Jenabian et al., 2010; Pineton de Chambrun et al., 2015). In addition, administration of the *S. cerevisiae* minimized the hepatic toxicity in broiler chickens (Poloni et al., 2020).

This investigation was aimed to evaluate the antioxidant, anti-inflammatory, and anti-apoptotic mechanisms of fermented garlic extract (FGE) against whole-body γ-irradiation induced brain and liver toxicity.

Materials and Methods

Chemicals

Fresh garlic was obtained from a local market. *S. cerevisiae* (ATCC 201390/ BY4743) was obtained from Microbiology Call resources Center (Cairo MIRCEN). All other chemicals were of the highest commercially available analytical grade and purchased from Sigma–Aldrich.

Preparation of fermented garlic extract

Fresh garlic was used in the present study. An aqueous extract of garlic was prepared using freshly peeled garlic cloves which were

homogenized in double-distilled water. The homogenate was centrifuged at 3000 rpm for 10 min to remove the particles. Then the garlic extract was fermented with edible *S. cerevisiae* (ATCC 201390 / BY4743) by 2-stage cultivation. At the first stage, the microorganism was cultivated in a medium containing 3% (wt/vol) malt extract for 36 hours at 28°C to enhance the cell growth. The cell mass was obtained by centrifugation at 3000 rpm for 10 min and re-cultivated in a medium containing 5% (wt/vol) of the garlic extracts. The fermented garlic extract was evaporated tell dryness at 50°C, and stored at 4°C. The residue was dissolved in distilled water before use to produce an equivalent daily use of 50 mg/kg.b.wt (Jung et al., 2011).

Radiation facility

A whole-body gamma-irradiation was performed at the National Center for Radiation Research and Technology (NCRRT), Atomic Energy Authority, Cairo, Egypt, using Canadian Gamma Cell-40 (^{137}Cesium), manufactured by the Atomic Energy of Canada Limited, Ontario, Canada. The radiation dose rate was 0.671 rad/sec at the time of exposure. The total radiation dose was 6 Gray (Gy) as a single dose whole body.

Experimental animals

Male *Wistar* rats (weighing 110–120 g) were obtained from the animal house breading unit, at National Center for Radiation Research and Technology (NCRRT), Nasr City, Cairo, Egypt. The animals were housed at the animal facility, at the NCRRT and allowed to acclimatize for one week before starting the experiment. The animals were kept under standard laboratory conditions of light/dark cycle (12/12 h), a temperature of 25±2°C, and humidity of 60±5% with free access to food and drinking water ad *libitum*. They were provided with a nutritionally adequate standard laboratory (pellet) diet. The study was conducted in accordance with international guidelines for animal experiments and approved by the Ethical Committee at the NCRRT, Atomic Energy Authority, Cairo, Egypt (27A/18).

Eexperimental design

The rats were divided into four groups (6 animals per group), Group I (C; control group), Group II (FGE), III (R: irradiated rats), Group IV (FGE+R). In C, and R groups rats administered orally with 1 ml of water. However, in FGE, and FGE+R groups, rats administered orally with 1 ml of FGE at a daily dose equivalent to 50 mg/kg.b.wt. (Jung et al., 2011). At day 21, R and FGE+R groups were exposed to a single shot of a whole-body gamma irradiation (6 Gy). After 24 h of radiation exposure and overnight fasting period with free access to water, the animals were sacrificed under urethane anesthesia, and the blood was withdrawn intra-cardiac. The blood was collected in EDTA-free-tubes, allowed to clot, centrifuged at 1200 *g* using universal centrifuge (16R, Germany), then sera were separated, and used for assessment of different biochemical parameters. Brain, and liver of each animal were excised immediately, then washed with physiological saline, and de-ionized water. Each tissue sample was divided into four parts: the cytosolic fraction was isolated from the first part and was used for the determination of the activities of the antioxidant enzymes (SOD, GSH-Px), and trace elements. The second part was homogenized in ice cold phosphate-buffered saline (10% w/v) for the determination of of MDA level, GSH contents, and caspase-3 activity. The third part was used for the determination of IL-1β, TNF-α, IL-6 levels by Enzyme-Linked Immunosorbent Assay (ELISA) kits, the relative gene expression ratio of NF-B, and STAT3 by RT-PCR, as well as, for the assessment of DNA fragmentation by gel-electrophoresis method. Tissues were stored at -80°C. In addition, brain and liver tissue samples of the fourth part were collected in 10% formalin for histopathological investigations.

Biochemical analysis

Assay of blood biochemical parameters

Biochemical parameters: Alanine and Aspartate Aminotransferase (ALT & AST, U/L), Alkaline Phosphatase (ALP, U/L), Gamma Glutamyl Transferase (GGT, U/L) activities, total cholesterol (TC, mg/dL) and triglycerides (TG, mg/dL) levels were determined in serum according to the manufacturer's instruction of the commercially available RANDOX kits.

Isolation of cytosolic fraction

The cytosolic fraction was isolated from brain or liver tissues according to Timmons et al. (2011). Approximately 1 g of brain tissues was homogenized in 9 ml of isolation buffer (IB), which is composed of: 10 mM Tris, 0.32M of sucrose, and 0.25 mM Na_2EDTA, at pH 7.4. Then the homogenates were centrifuged at 2000 g, for 3 min, at 4°C. The supernatant was collected and the pellet re-suspended in approximately half the

original volume of IB, then re-homogenized and centrifuged (2000 g, 3 min, 4◦C). The combined supernatants from steps 2 and 3 were centrifuged (20,000×g, 10 min, at 4◦C). The final supernatant was kept at -20ºC as the crude cytosolic fraction. The total protein concentrations in the brain and liver tissues and their cytosolic fractions were estimated by Lowry's method (Lowry et al., 1951).

Assay for antioxidant and oxidative stress parameters

Estimation of super oxide dismutase (SOD): The cytosolic homogenates were extracted with 0.25 ml chloroform and 0.5 ml ethanol followed by vigorous mixing. The clear supernatant produced after centrifugation (12000 *xg*, 4°C for 60 min) was used for the SOD assay. The assay was performed according to the method of Minami & Yoshikawa (1979). This method is based on the generation of superoxide anions by pyrogallol autoxidation, detection of the generated superoxide anions by nitroblue tetrazolium dye, and finally measurement of the amount of generated superoxide anions scavenged by SOD at 560 nm. The enzyme activity was expressed as U/mg protein.

Estimation of glutathione-peroxidase (GSH-Px): GSH-Px activity was measured in the cytosolic fractions according to Rotruck et al. (1973). The assay is based on the indirect determination of GSH-Px, whereas GSH-Px react with known amount of GSH, then the residual glutathione reacted with DTNB (Dithio Nitrobenzoic acid). The color developed was read at 412 nm. The enzyme activity was expressed as µ moles of GSH oxidized/mg protein/min (U/mg protein).

Determination of glutathione reduced level (GSH): GSH content was measured according to Ellman (1959). After precipitation of proteins by trichloroacetic acid (TCA), the glutathione in the brain or liver homogenates was reacted with DTNB (5-5'-dithionitrobenzoic acid; Sigma) to yield the yellow chromophore of TNB (thio nitrobenzoic acid acid), which was measured at 412 nm. GSH (Sigma) was used as standard. GSH concentration was expressed as µg/mg Protein.

Determination of malondialdehyde (MDA): Lipid peroxides in terms of malondialdehyde (MDA) were measured in the brain and liver tissues according to the method of Satoh (1978). The assay depends on the colorimetric reaction of MDA with thiobarbituric acid giving a pink complex that can be measured at 532 nm. MDA contents were expressed as nmol/mg protein.

Detection of tumor necrosis factor alpha, interleukin-1 beta, and Interleukin-6

TNF-α, IL-1β, and IL-6 were determined in the serum, using ELISA kits for rat. Measurements were done according to the catalogue-instruction guidelines. Cytokine levels were calculated after plotting the standard curves and expressed as pg/ml.

Detection of nuclear factor kappa B and signal transducer and activator of transcription-3 relative gene expression ratio in brain and liver tissues by quantitative real time PCR (qRT-PCR):

The total RNA from the frozen brain and liver tissues were extracted by a Qiagen kit (USA), which was then isolated, and then inversely transcript into the complementary DNA (cDNA) by Moloney murine leukemia virus (M-MLV) reverse transcriptase (Promega, Madison, USA). Step One Plus Real-Time PCR System (Applied Biosystems, Foster City, CA, USA) and an SYBR® Green PCR Master Mix (Applied Biosystems) were conducted in a 10 µl final volume, programming the heating cycles: 95°C (10 min), then 40 cycles of 95°C (15 s) and 65°C (1 min). The sequences of PCR primer pairs with the corresponding bank gene accession number of NF-κB Forward: 5′- GCT TAC GGT GGG ATT GCA TT -3′, Reverse: 5′-TTA TGG TGC CAT GGG TGA TG-3′, STAT3: Forward: 5′-CAA AGA AAA CAT GGC CGG CA-3′, Reverse: 5′-GGG GGC TTT GTG CTT AGG AT-3′, and glyceraldehyde 3-phosphate dehydrogenase (GAPDH): forward 5'-AGT TCA ACG GCA CAG TCA AGG-3', reverse: 5'-AGA CTC CAC GAC ATA CTC AGC-3'. The results were evaluated by the ABI Prism sequence detection system software and computed using v1.7 Sequence Detection Software, from PE Biosystems (Foster City, CA). The relative expression values of the studying genes were evaluated using the comparative threshold cycle method. All values were normalized to GAPDH gene, applying the expression 2-ΔΔCt (Livak and Schmittgen, 2001).

Detection of caspase-3 activity

Caspase-3 was measured in brain or liver

homogenates using rat caspase-3 ELISA kit (MyBiosource, USA Cat No.: MBS261814), according to the manufacturer's instruction. The experiments were repeated three times and caspase-3 concentrations were expressed as ng/ml.

DNA fragmentation analysis

For the determination of genomic DNA fragmentation, rat brains were rapidly removed, washed, and homogenized. The homogenized tissue was transferred to a centrifuge tube with extraction buffer (10 mmol/L Tris-HCl (pH 8.0), 0.1 mol/L EDTA (pH 8.0) and 0.5% SDS, then incubated for 1 hour at room temperature and then digested in the same buffer with 200 µg/ml proteinase K (Sigma) at 50°C overnight. An equal volume of phenol equilibrated with 1 mol/L Tris buffer (pH 8.0) was then added, and the tube was placed on a roller apparatus for 1 h. After the two phases were separated by centrifugation at 5000 g for 30 min at room temperature, the viscous aqueous phase was transferred to a clean tube, and the extraction was repeated with an equal volume of phenol/chloroform. After the second extraction, the aqueous phase was separated and the DNA precipitated by addition of 0.1 vol 3 mol/L sodium acetate and 2 vol 100% ethanol. DNA precipitate was collected by centrifugation at 15000 g for 20 min at room temperature, rinsed with 70% ethanol, and finally re-suspended in 0.5 ml extraction buffer in a 1.5-ml microcentrifuge tube until dissolved. To detect DNA fragmentation, 10 µl of each DNA was electrophoretically fractionated on 1.5% agarose gel with 0.5 µg/ml ethidium bromide then visualized and photographed under UV light (Okamura et al., 2000).

Determination of trace elements levels in the brain and liver tissues

The cytosolic fractions of brain and liver tissues from the different groups were digested in a mixture of concentrated nitric acid (HNO_3) and hydrogen peroxide (H_2O_2) (5:1 v/v) until complete digestion of the organic materials using Milestone MLS-1200 Mega, High Performance Microwave Digester Unit, Italy (NCRRT). The level of the trace elements; namely iron (Fe), calcium (Ca), copper (Cu), magnesium (Mg), manganese (Mn) and zinc (Zn) were estimated in the prepared samples using Atomic Absorption spectrophotometer (Thermo Scientific, iCE 3000, England), at the NCRRT, Atomic Energy Authority, Nasr City, Cairo, Egypt.

Histopathological investigations

For histopathological investigations, brain and liver tissue samples were fixed in a 10% neutral buffered formalin solution. Tissue samples were dehydrated in scaling ethanol concentration, washed with xylene, immobilized in paraffin wax, and split at a 5-micron thickness, then stained by hematoxylin and eosin (H&E) on glass slides (Bancroft & Layton, 2019).

Statistical analysis

All statistical analyses were conducted using the statistical package for Windows Version 23 (SPSS Software, Chicago, IL). The results for continuous variables were expressed as mean±standard error. Values were compared by one-way analysis of variance (ANOVA). Post hoc testing was performed for inter-group comparisons, using the least significant difference (LSD) test. Significance of P value < 0.05 was considered statistically significant, while significance of P value < 0.01 was considered highly significant.

Results

Biochemical parameters

As a result of 6 Gy of gamma-radiation exposure (R, group III), highly significant elevation ($P<0.01$) in the serum hepatic enzymes activities; ALT (2.5 folds), AST (2 folds), ALP (2.9 folds) and GGT (2.2 folds) was observed. Moreover, tthe serum levels of TC and TG revealed high significant elevations by 2.6 and 1.5 folds, respectively, as compared to the untreated control animals ($P<0.01$). The data in the group IV (FGE +R) revealed a significant amelioration of these biochemical markers towards the normal levels (Table 1).

Antioxidant status in the brain and the liver tissues

Superoxide dismutase

Table 2 shows that SOD activities in the cytosolic fraction of the brain and liver tissues were significantly decreased ($P<0.01$) to 84.0% and 76.0%, respectively, in brain and liver tissues of γ-irradiated animals (R, group III), as compared to the control group. FGE pre-treatment of rats exposed to whole body γ-radiation (FGE+R, group IV) significantly elevated the observed changes in the SOD activities in the cytosolic fraction of the brain and liver tissues, as compared to the control values.

TABLE 1. Effect of fermented garlic extract administration on different biochemical parameters in blood serum

Groups parameters	Control (C, group I)	Fermented garlic extract (FGE, group II)	γ-irradiation (R, group III)	Fermented garlic extract + γ-irradiation (FGE+R, group IV)
Alanine Aminotransferase (U/L)	45.33 ± 3.41	42.17 ± 1.49	116.67 ± 6.83 [a]	51.17 ± 1.64[a,b]
Aspartate Aminotransferase (U/L)	117.83 ± 4.19	244.83 ± 8.54	114.00 ± 4.93 [a]	134.67 ± 2.83 [a,b]
Alkaline phosphatase (U/L)	139.00 ± 2.56	155.33 ± 1.82	402.67 ± 18.64 [a]	176.33 ± 4.84 [a,b]
Gamma-glutamyl transferase (U/L)	5.0 ± 0.21	5.83 ± 0.84	11.0 ± 0.45 [a]	5.83 ± 0.83 [b]
Total cholesterol (mg/dL)	45.33 ± 3.41	42.17 ± 1.49	116.67 ± 6.85 [a]	50.33 ± 2.60 [a,b]
Triglycerides (mg/dL)	86.86 ± 3.41	91.33± 2.98	141.00 ± 2.40 [a]	103.84 ± 1.45 [a,b]

The results are expressed as Mean ± SE (n =6). a: Significance versus control, b: Significance versusγ-irradiated group , at P<0.01.

TABLE 2. Effect of fermented garlic extract on antioxidants in the cytosolic fractions of brain and liver tissues of γ-irradiated rats

Groups	Superoxide dismutase U/ mg protein		Glutathione peroxidase U/ mg protein	
	Brain	Liver	Brain	Liver
Control (C, group I)	13.28 ± 0.203	11.64 ± 0.35	4.42 ± 0.06	6.18 ± 0.82
Fermented garlic extract (FGE, group II)	11.97 ± 0.552	11.30 ± 0.297	4.21± 0.07	5.89 ± 0.62
γ-irradiation (R, group III)	11.23 ± 0.139 [a]	8.82 ± 0.90 [a]	1.27 ± 0.09 [a]	1.78 ± 0.74 [a]
Fermented garlic extract + γ-irradiation (FGE+R, group IV)	13.16 ± 1.167 [a,b]	11.26 ± 0.6 [a,b]	3.40 ± 0.08 [a,b]	4.75 ± 0.41 [a,b]

The results are expressed as Mean ± SE (n = 6).a: Significance versus control, b: Significance versus γ-irradiated group, at P<0.01.

Glutathione peroxidase

Activity of GSH-Px was measured in the cytosolic fraction of the brain and liver tissues of different studied groups (Table 2). The GSH-Px enzyme activities were decreased considerably (P< 0.001) to 28.7% and 28.8%, respectively, in the cytosolic fraction of the brain and liver tissues of γ-irradiated animals (R, group III), as compared to the control group. However, FGE pre-treatment of γ-irradiated rats (FGE +R, group IV) significantly maintains the activities of GSH-Px in cytosolic fraction of the brain and liver tissues.

Lipid peroxidation

The most widely used test for oxidative stress is the measurement of MDA, a product of LPO, by the thiobarbituric acid reacting substances assay. LPO level appeared to be remarkably enhanced; as evidenced by increased production of MDA in the brain and liver tissues' homogenates of γ-irradiated rats (R, group III) by 1.9 and 2.6 folds, respectively, as compared to the corresponding normal values. FGE pre-treatment significantly minimized the elevated MDA levels in the brain and liver tissues of γ-irradiated animals (FGE +R, group IV) (Table 3).

Glutathione reduced

The level of GSH was measured in brain and liver tissues of different studied groups (Table 3). GSH level was significantly depleted (P<0.01) to 59.3% and 62.1%, respectively in the brain and liver tissues of γ-irradiated animals (R, group III), as compared to the normal animals. FGE pre-treatment significantly regulated GSH levels in the brain and liver tissues of γ-irradiated animals (FGE+R, group IV) towards the control levels.

TABLE 3. Effect of fermented garlic extract on malondialdehyde and glutathione levels in the brain and liver tissues of γ-irradiated rats

Groups	Malondialdehyde nmol/mg protein		Glutathione reduced µg/mg protein	
	Brain	Liver	Brain	Liver
Control (C, group I)	90.6 ± 4.739	84.66 ± 8.45	12.38 ± 0.17	13.82 ± 0.29
Fermented garlic extract (FGE, group II)	122.4 ± 12.09	119.6 ± 4.68	10.72 ± 0.21	11.86 ± 0.51
γ-irradiation (R, group III)	171.5 ± 9.005 [a]	216.3 ± 21.63[a]	7.34 ± 0.20 [a]	8.58 ± 0.59 [a]
Fermented garlic extract + γ-irradiation (FGE+R, Group IV)	136.6 ± 5.697 [a,b]	154.6 ± 13.25[a,b]	9.68 ± 0.18 [a,b]	11.12 ± 0.18[a,b]

The results are expressed as Mean ± SE (n = 6).a: Significance versus control, b: Significance versus γ-irradiated group, at P<0.01.

Pro-inflammatory markers: Tumor Necrosis Factor alpha, Interleukin-1 beta,Interleukin-6

Pro-inflammatory cytokines, including TNF-α, IL-1β, and IL-6 were induced in the brain and liver tissues by ionizing radiation. Exposure of rats to a whole body γ-radiation (6 Gy, R, group III) resulted in high significant elevations (P<0.01) of TNF-α, IL-1β and IL-6 levels, as compared to the control animals; as shown in Table 4. TNF-α levels were enhanced by 3.84 and 2.87 folds, , IL-1β levels were increased to 5.85 and 2.67, and, and IL-6 levels were amplified by 3.1 and 3.6 folds, respectively, in the brain and liver tissues of γ-irradiated animals. While, IL-6 was increased by 3.1 and 3.6 folds respectively in the brain and liver tissues of γ-irradiated animals. However, FGE pretreatment of γ-irradiated animals (FGE+R, group IV) significantly attenuated the increase of TNF-α, IL-1β and IL-6 levels, as compared to the corresponding control values (Table 4).

Nuclear factor kappa B and signal transducer and activator of transcription 3 relative gene expression levels

The relative gene expression levels of nuclear factor kappa B (NF-κB) and signal transducer and activator of transcription 3 (STAT3) were up-regulated in the brain and liver tissues in rats exposed to ionizing radiation (R, group III). Exposure of rats to a whole body γ-radiation (6 Gy) resulted in a high significant up-regulation of NF-κB relative gene expression ratios (P<0.01) by 7.6 and 7.9 folds, while STAT3 gene expression ratios were up-regulated by 7.5 and 8.3 folds, respectively in the brain and liver tissues of γ-irradiated animals. However, pretreatment of γ-irradiated animals (FGE+R, group IV) by FGE significantly down-regulated the elevated relative gene expression levels of NF-κB and STAT3 towards their corresponding normal levels (Fig. 1).

TABLE 4. Effects of fermented garlic extract on the levels of tumor necrosis factor-α, interleukin-1 β, and interleukin-6 in brain and liver of γ-irradiation rats

Groups	Tumor necrosis factor-α (TNF-α, pg/ml)		Interleukin-1β (IL-1β, pg/ml)		Interleukin-6 (IL-6, pg/ml)	
	Brain	Liver	Brain	Liver	Brain	Liver
Control (C, group I)	26.5±2.3	30.7±1.0	11.6±1.1	29.4±2.8	31.07±1.7	30.07±1.3
Fermented garlic extract (FGE, group II)	31.4±3.0	28.8±2.0	21.7±2.5	24.1±2.2	42.4± 1.8	46.3±4.3
γ-irradiation (R, group III)	91.1±3.4[a]	102.8±6.3[a]	75.2±5.5 [a]	76.0±3.2[a]	97.2±2.5[a]	104.3±3.2[a]
Fermented garlic extract + γ-irradiation (FGE+R, group IV)	56.9±4.0[a,b]	63.5±4.5[a,b]	38.1±2.4[a,b]	47.8±2.7 [a,b]	50.17±2.2 [a,b]	54.6±2.5 [a,b]

The results are expressed as Mean ± SE (n = 6). a: Significance versus control, and b: Significance versus γ-irradiated group, at P<0.01.

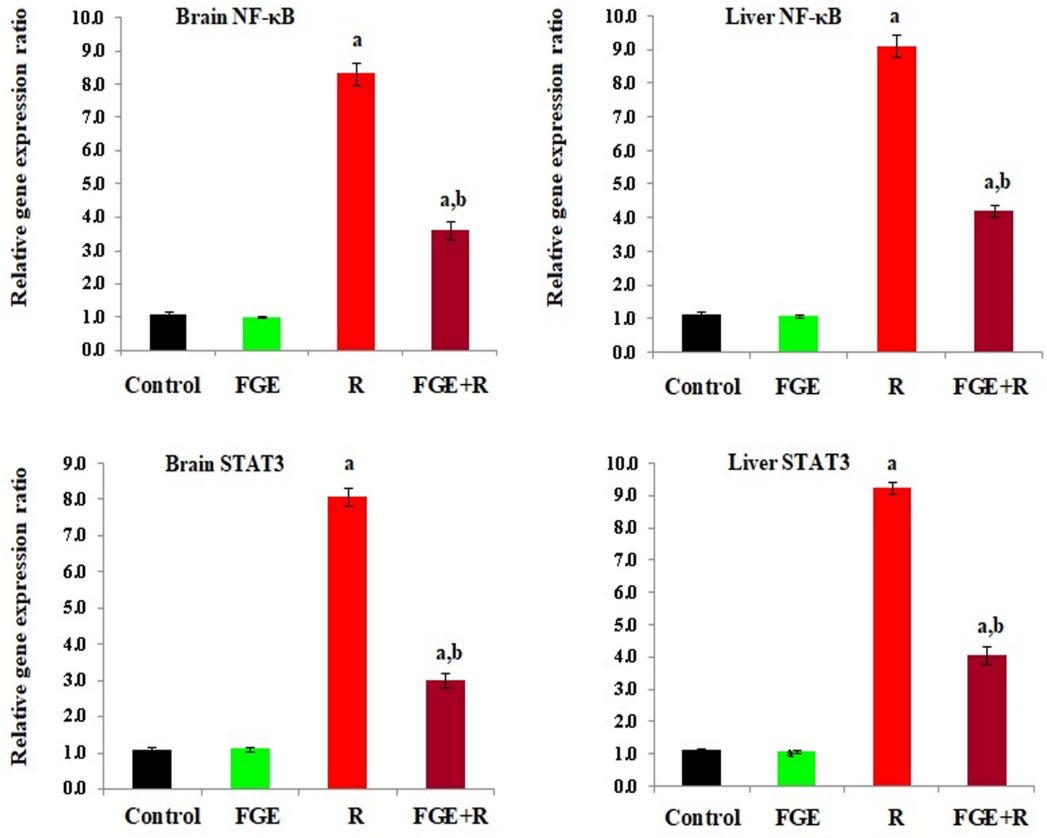

Fig. 1. Relative gene expression ratio of NF-κB and STAT3 in brain and liver tissues of different experimental groups [The results are expressed as Mean ± SE (n = 6); a: Significance versus control, and b: Significance versus γ-irradiated group, at P<0.01]

Caspase-3

The level of caspases-3 was measured in brain and liver tissues of different studied groups. Caspase-3 activities were significantly increased (P<0.001) to 3.5 and 3.4 folds, respectively in the brain and liver tissues of γ-irradiated animals (R, group III) as compared to the normal animals. FGE pre-treatment decreased caspase-3 activities in the brain and liver tissues of γ-irradiated animals (FGE+R, group IV) to 1.8 and 2.1 folds, respectively, as compared to controls (Fig 2).

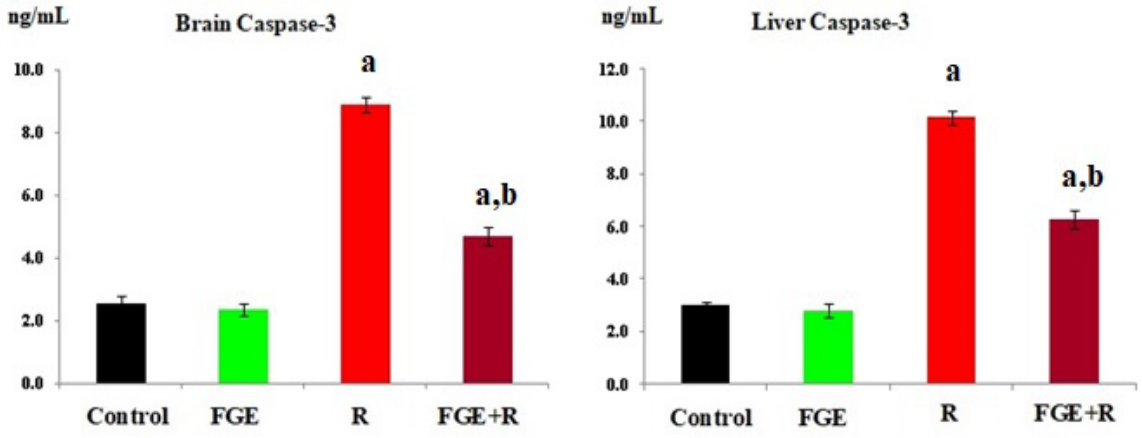

Fig. 2. Caspase-3 level determined by Rat ELISA kits in brain and liver tissues of different experimental groups [The results are expressed as Mean ± SE (n = 6); a: Significance versus control, and b: Significance versus γ-irradiated group, at P< 0.01]

DNA fragmentation

The DNA fragmentation pattern was monitored in the brain and liver tissues of the different experimental groups by agarose gel electrophoresis. The γ-irradiated group (R, group III) showed strand breaks/ streaking of DNA (as opposed to low molecular weight bands specific to apoptosis) which was undetected in the DNA isolated from the control (group I) and treated groups (FGE, group II & FGE+R, group IV) that showed presence of undamaged DNA (Fig. 3).

Trace elements

Figures 4 and 5 demonstrate that gamma-irradiation induced alteration in the levels of some trace elements. Levels of Ca, Fe, and Cu were elevated, but Mg, Mn and Zn levels were declined in the cytosolic fractions of the brain and liver of gamma-irradiated rats (R, group III). FGE-pretreatment of gamma-irradiated rats conserves the level of the trace elements under investigation as compared to their corresponding normal values.

Histopathological investigations

Brain Histopathological results:

The brain tissues of the control group (group I) and fermented garlic extract (FGE, group II) treated groups showed average meninges, average cerebral cortex with average neurons and average glial cells and average intra-cerebral blood vessels, and striatum with average neurons and average glial cells and average intra-cerebral blood vessels (Fig. 6a &6b). Hippocampus showed average Cornu Amonis (CA1), (CA2), (CA3), average dentate gyrus (DG), average pyramidal neurons, average inter-neuron areas, and average blood vessels (Fig. 6c &6d). The brain of gamma-irradiated group (R, group III) showed average meninges, cerebral cortex with markedly degenerated neurons, average glial cells, mildly congested blood vessels and eosinophilic plaque-like areas, and striatum with markedly degenerated neurons, average glial cells and eosinophilic plaque-like areas (Fig. 7a &7b). Hippocampus showed markedly degenerated pyramidal neuronsin Cornu Amonis (CA3), scattered degenerated pyramidal neurons in (CA1) and (CA2), average dentate gyrus (DG), average inter-neuron areas, and average blood vessels (Figs. 7c &7d, 7f & 7g). The brain of the FGE treated group exposed to gamma-irradiation (FGE+R, group IV) showed average meninges, cerebral cortex with scattered degenerated neurons, average glial cells and average blood vessels, and striatum with average neurons, average glial cells and average blood vessels (Fig. 8a). Hippocampus showed markedly degenerated pyramidal neuronsin Cornu Amonis (CA1), scattered degenerated pyramidal neurons in (CA2), (CA2), and in (DG), average inter-neuron area, and average blood vessels (Fig 8b, & 8c). Tables 5 and 6 showed the histopathological scoring of the brain Cortex and Striatum as well as brain hippocampus, respectively, in normal and γ-irradiated rats treated with FGE.

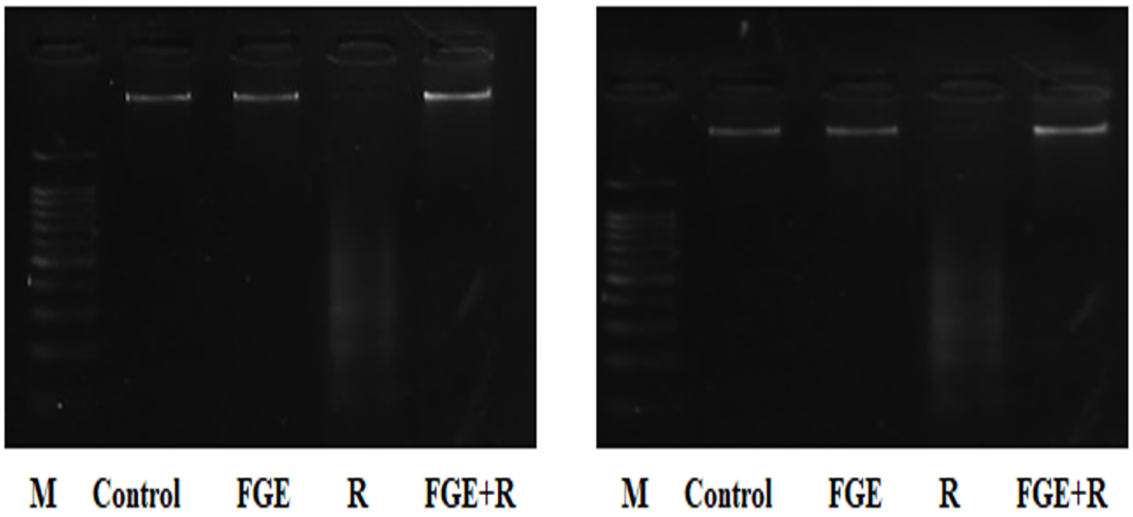

Fig. 3. Agarose gel electrophoresis of DNA isolated from brain and liver homogenates [Lane M: DNA marker with 100bp, Lane 1: C (Control group), Lane 2: FGE (Fermentedgarlic extract treated group), Lane 3: R (γ-irradiation treated group), Lane 4: FGE+R: (Fermented garlic extract + γ-irradiation treated group)]

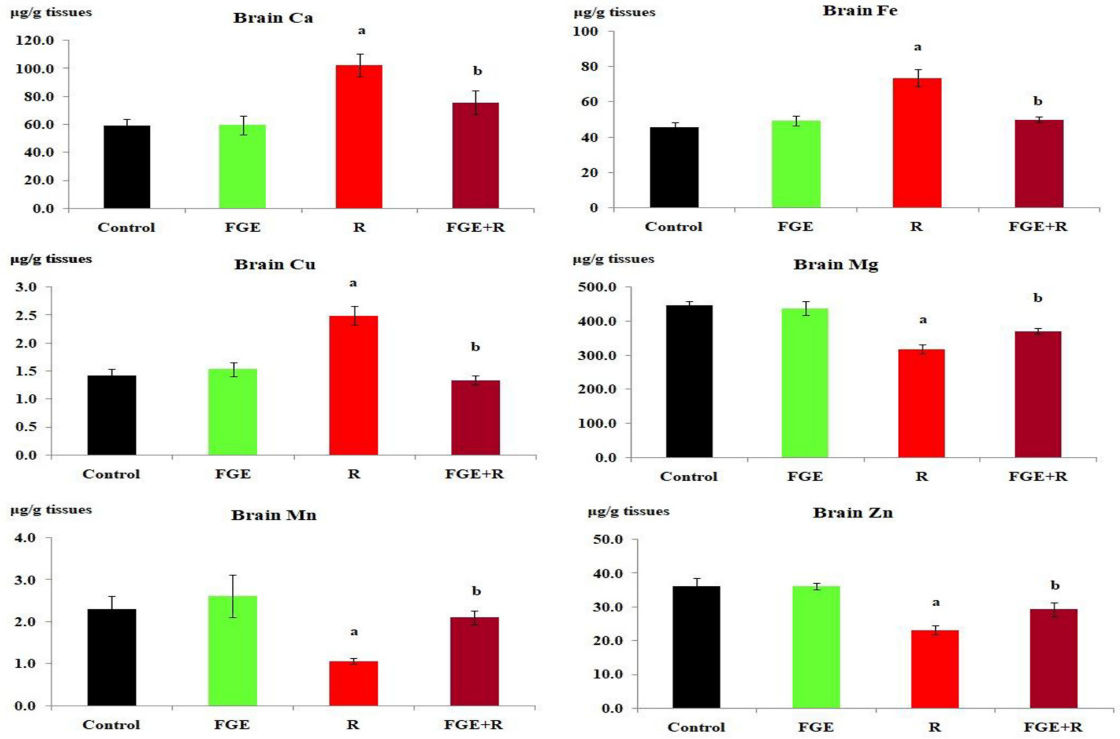

Fig. 4. Trace elements levels in the cytosolic fractions of the brain tissues of different experimental groups [The results are expressed as Mean ± SE (n = 6); a: Significance versus control, and b: Significance versus γ-irradiated group, at P<0.01]

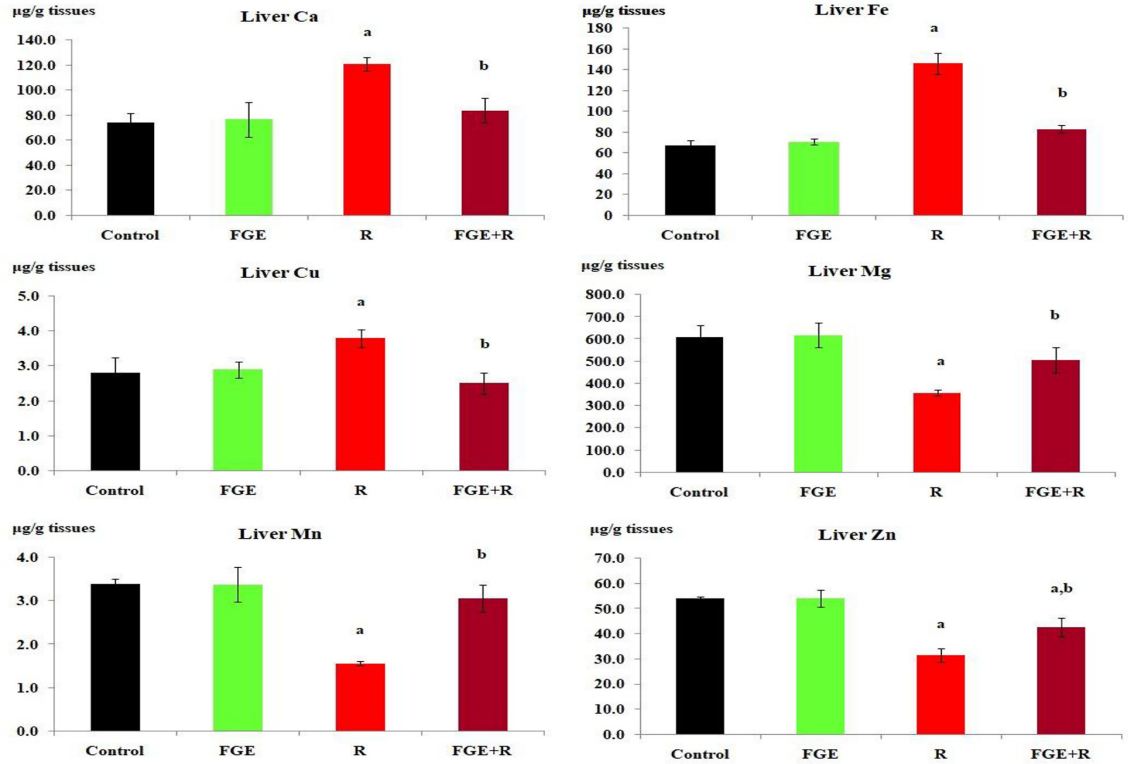

Fig. 5. Trace elements levels in the cytosolic fractions of the liver tissues of different experimental groups [The results are expressed as Mean ± SE (n = 6); a: Significance versus control, and b: Significance versus γ-irradiated group, at P<0.01]

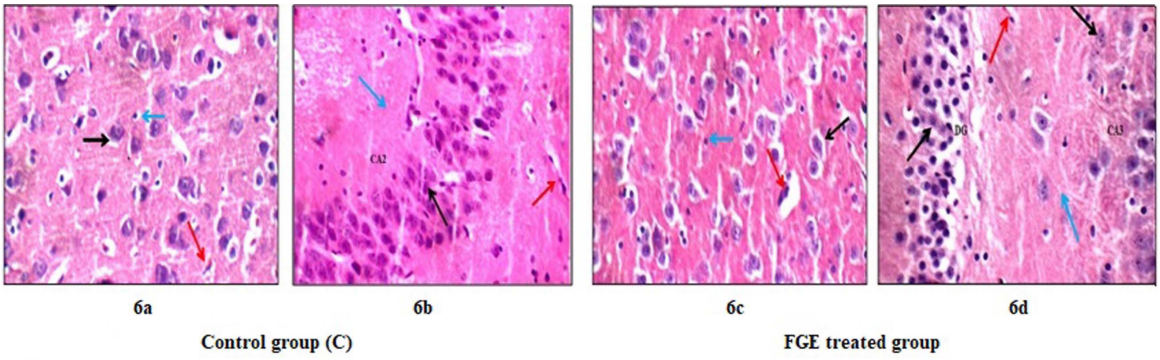

Fig. 6. showing normal brain structure of the control and fermented garlic extract (FGE) treated groups. Fig 6a: Control group: deep cortex view showing average neurons (black arrow), average glial cells (blue arrow), and average intra-cerebral blood vessels (red arrow) (H&E X 400), Fig 6b: Control group: another view in (CA2) showing average pyramidal neurons (black arrow), average inter-neuron area (blue arrow), and average blood vessels (red arrow) (H&E X 400), Fig 6c: Fermented garlic extract treated group: striatum showing average neurons (black arrow), average glial cells (blue arrow), and average intra-cerebral blood vessels (red arrow) (H&E X 400), Fig 6d: Fermented garlic extract treated group: (CA3) and in (DG) showing average pyramidal neurons (black arrow), average inter-neuron area (blue arrow), and average blood vessels (red arrow) (H&E X 400)

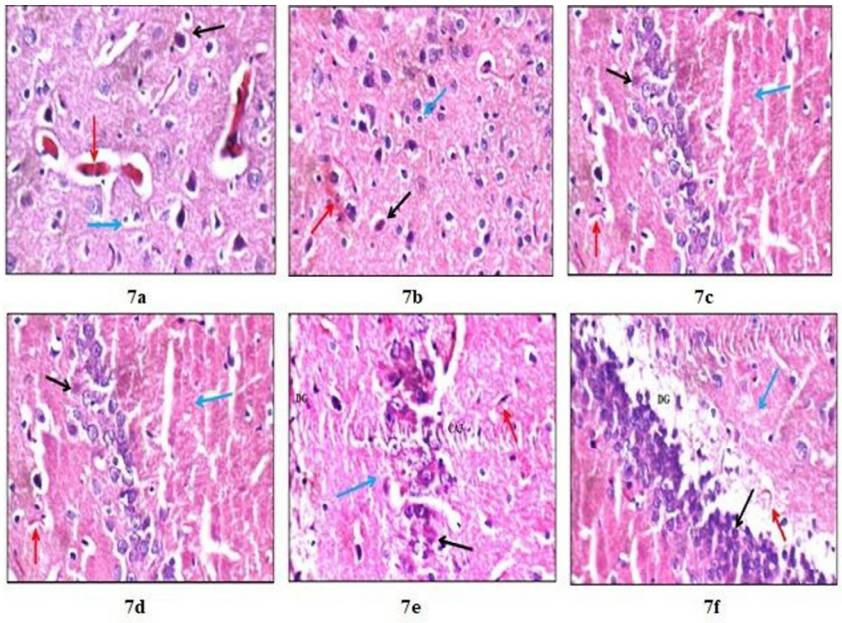

Fig. 7. Showing the histopathological changes of gamma-irradiated rats' brain, revealed average meninges, cerebral cortex with markedly degenerated neurons, average glial cells, mildly congested blood vessels and eosinophilic plaque-like areas, and striatum with markedly degenerated neurons, average glial cells and eosinophilic plaque-like areas. Fig 7a: Gamma-irradiated group: brain showing markedly degenerated neurons (black arrow), average glial cells (blue arrow), and mildly congested blood vessels (red arrow) (H&E X 400). Fig 7b: Gamma-irradiated group: another view in striatum showing markedly degenerated neurons (black arrow), average glial cells (blue arrow), and eosinophilic plaque-like area (red arrow) (H&E X 400). Fig 7c: Gamma-irradiated group: hippocampus higher power view in (CA1) showing scattered degenerated pyramidal neurons (black arrow), average inter-neuron area (blue arrow), and average blood vessels (red arrow) (H&E X 400). Fig 7d: Gamma-irradiated group: hippocampus higher power view in (CA2) showing scattered degenerated pyramidal neurons (black arrow), average inter-neuron area (blue arrow), and average blood vessels (red arrow) (H&E X 400). Fig 7e: Gamma-irradiated group: hippocampus (CA3) showing markedly degenerated pyramidal neurons (black arrow), average inter-neuron area (blue arrow), and average blood vessels (red arrow) (H&E X 400). Fig 7f: Gamma-irradiated group: another view in (DG) showing average pyramidal neurons (black arrow), average inter-neuron area (blue arrow), and average blood vessels (red arrow) (H&E X 400)

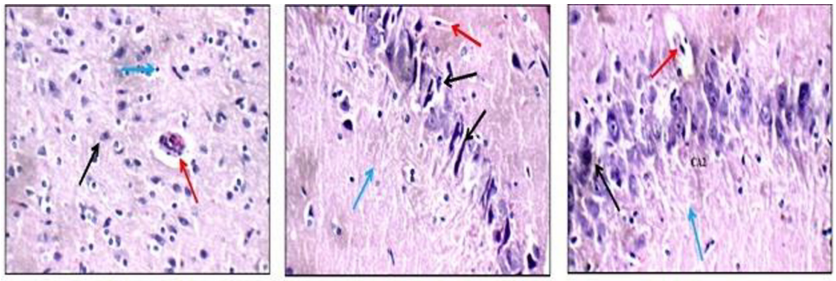

8a 8b 8c

Fig. 8. Brain showed average meninges, cerebral cortex with scattered degenerated neurons, average glial cells and average blood vessels, and striatum with average neurons, average glial cells and average blood vessels, Fig. 8a: Fermented garlic extract treated group exposed to gamma-irradiation: striatum showing average neurons (black arrow), average glial cells (blue arrow), and average intra-cerebral blood vessels (red arrow) (H&E X 400). Hippocampus showe dmarkedly degenerated pyramidal neurons in Cornu Amonis (CA1), scattered degenerated pyramidal neurons in (CA2), (CA2), and in (DG), average inter-neuron area, and average blood vessels. Fig. 8b: Fermented garlic extract treated group exposed to gamma-irradiation: hippocampus higher power view in (CA1) showing markedly degenerated pyramidal neurons (black arrow), average inter-neuron area (blue arrow), and average blood vessels (red arrow) (H&E X 400). Fig. 8c: Fermented garlic extract treated group exposed to gamma-irradiation: (CA2) showing scattered degenerated pyramidal neurons (black arrow), average inter-neuron area (blue arrow), and average blood vessels (red arrow) (H&E X 400)

TABLE 5. Histopathological scoring of the brain cortex and striatum in normal and γ-irradiated rats treated with fermented garlic extract

Group	Cortex					Striatum			
	Meninges	Neurons	Glial cells	BV	Back-ground	Neurons	Glial cells	BV	Back-ground
Control (C, group I)	0	0	0	0	0	0	0	0	0
Fermented garlic extract (FGE, group II)	0	0	0	0	0	0	0	0	0
γ-irradiation (R, group III)	0	++	0	+	+	++	0	0	+
Fermented garlic extract + γ-irradiation (FGE+R, group IV)	0	+	0	0	0	0	0	0	0

- Meninges: 0: Average, +: Detached, ++: Markedly thickened.
- Neurons: 0: Average, +: Scattered degenerated, ++: Markedly degenerated.
- Glial cells: 0: Average, +: Scattered degenerated, ++: Markedly degenerated.
- BV: 0: Average, +: Dilated/congested, ++: Markedly dilated.
- Background: 0: Average, +: Eosinophilic plaque-like areas, ++: Areas of necrosis/Hge/calcification.

TABLE 6. Histopathological scoring of the brain hippocampus in normal and γ-irradiated rats treated with fermented garlic extract

Group	Hippocampus					
	CA1	CA2	CA3	DG	Inter-neuron area	BV
Control (C, group I)	0	0	0	0	0	0
Fermented garlic extract (FGE, group II)	0	0	0	0	0	0
γ-irradiation (R, group III)	+	+	++	0	0	0
Fermented garlic extract + γ-irradiation (FGE+R, group IV)	++	+	+	+	0	0

- Pyramidal neurons: 0: Average, +: Scattered degenerated, ++: Markedly degenerated.
- Inter-neuron area: 0: Average, +: Edema/hemorrhage, ++: Eosinophilic plaque-like areas.
- BV: 0: Average, +: Dilated/congested, ++: Markedly dilated.

Liver histopathological investigations:

The liver of the control group (group I) and fermented garlic extract (FGE, group II) treated groups showed average portal tracts with average portal veins and average hepatocytes in peri-portal area, and average central veins with average hepatocytes arranged in single-cell cords with average intervening blood sinusoids (Fig. 9a, &9b). The liver of the gamma-irradiated (R, group III) treated group showed average portal tracts with markedly dilated congested portal veins, markedly dilated central veins, and marked apoptosis with mild micro-vesicular steatosis of hepatocytes in peri-portal and peri-venular areas (Fig. 9c). The liver of the fermented garlic extract treated group exposed to gamma-irradiation (FGE+R, group IV) showed mildly edematous portal tracts with mildly dilated congested portal veins and average hepatocytes in peri-portal area, and mildly dilated central veins with average hepatocytes in peri-venular areas (Fig. 9d). Table 7 shows the histopathological scoring of the liver tissues in normal and γ-irradiated rats treated with FGE.

Discussion

In the current study, acute gamma-radiation exposure demonstrates alterations in the biochemical parameters, highly significant elevations of the hepatic marker enzymes; ALT, AST, ALP, and GGT activities, as well as, TC, and TG levels in the blood serum were observed. Similar results were recorded by investigators (Salem et al., 2016). The disturbance in the liver function could be attributed to the gamma-irradiation that triggers oxidative stress, and enhances the release of free radicals, which alter the activity of the hepatic enzymes and lipid metabolism. The released free radicals attack the unsaturated fatty acids of the hepatic cell membranes, initiate lipid peroxidation (LPO), causing membrane incompetence, and then reduce the membrane fluidity. The increase in aminotransferase (ALT & AST), ALP and GGT activities by radiation exposure could be attributed to the hepatocytes cellular membranes destruction and dysfunction after exposure to acute whole body gamma-irradiation, which consequently leads to increased permeability of cell membranes, facilitating cytoplasmic enzymes passage outside the cells, resulting in increased activities of amino-transferases in the serum (Salem et al., 2016). Additionally, the oxidative stress in gamma-irradiated group can alter the hepatic lipid metabolism, and enhanced fat mobilization from adipose tissues due to cellular bio-membranes damage. The increased level of serum cholesterol fractions was probably due to its release from tissues, destruction of cell membranes and increase rate of cholesterol biosynthesis in the liver and other tissues. The increased level of TG occurred after γ-irradiation might be related to the decrease in lipoprotein lipase activity in adipose tissue, leading to a reduction in the uptake of triglycerides (Feurgard et al., 1998; Salem et al., 2016; Eassawy et al., 2021).

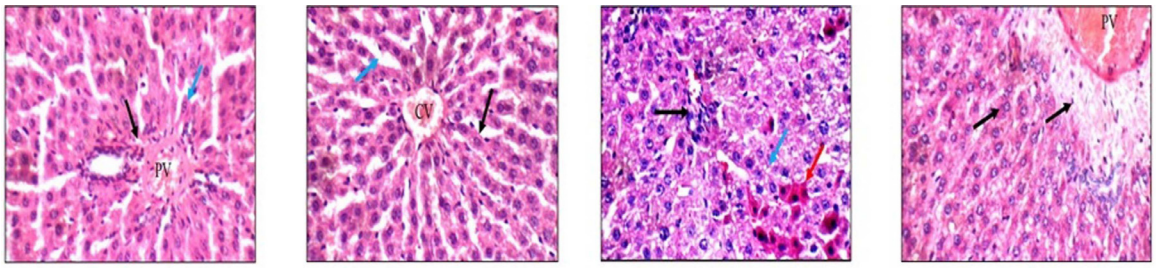

9a 9b 9c 9d

Fig. 9. Liver histopathological investigations of different treated group. Fig 9a: Control group: liver showing average portal tract (black arrow) with average portal vein (PV), and average hepatocytes in peri-portal area (blue arrow) (H&E X 400). Fig 9b: Fermented garlic extract treated group: liver showing average central vein (CV) and average hepatocytes arranged in single-cell cords (black arrow) with average intervening blood sinusoids (blue arrow) (H&E X 400). Fig 9c: Gamma-irradiated group: high power view showing average portal tract with average portal vein (black arrow), and marked apoptosis (red arrow) and mild micro-vesicular steatosis of hepatocytes in peri-portal area (blue arrow) (H&E X 400). Fig 9d: Fermented garlic extract treated group exposed to gamma-irradiation: showing mildly edematous portal tracts (black arrow) with mildly congested portal veins (PV), and average hepatocytes in peri-portal area (blue arrow) (H&E X 400)

TABLE 7. Histopathological scoring of the liver in normal and γ-irradiated rats treated with Fermented garlic extract

Group	Portal tract				Peri-venular area			
	PV	Inflammatory infiltrate	Edema	Hepatocytes	CV	Blood sinusoids	Hepatocytes	Inflammatory infiltrate
Control (C, group I)	0	0	0	0	0	0	0	0
Fermented garlic extract (FGE, group II)	0	0	0	0	0	0	0	0
γ-irradiation (R, group III)	++	0	0	++	++	0	++	0
Fermented garlic extract + γ-irradiation (FGE+R, group IV)	+	0	+	0	+	0	0	0

- **Portal tract:**
  - Portal vein (PV):0: Average +: Mildly dilated/congested++: Markedly dilated/congested
  - Inflammatory infiltrate:0: No +: Mild++: Moderate/marked
  - Edema :0: No +: Mild++: Moderate/marked
  - Hepatocytes: 0: Average +: scattered apoptosis/mild hydropic change ++: Marked apoptosis
- **Peri-venular area:**
  - Central vein:0: Average+: Mildly dilated/congested ++: Markedly dilated/congested
  - Blood sinusoids:: Average +: Mildly dilated/congested ++: Markedly dilated/congested
  - Hepatocytes:0: Average +: scattered apoptosis/mild hydropic change ++: Marked apoptosis

Exposure to gamma-radiation stimulates oxidative stress and inflammatory responses in the cells, in intricate closed cycle, as adaptive-responses to protect the cells and tissues. Oxidative stress and inflammation are two endless related processes, each one leads to the other. As a result, MDA is highly increased, the activity of the antioxidant enzymes, such as SOD and GSH-Px are altered, thus GSH contents diminished, accompanied with high levels of the pro-inflammatory markers, including TNF-α, IL-1β, IL-6 and NF-κB. This is what happened in the cytosolic-fractions of the brain and liver tissues of this investigation, which follows the pervious inspection of Ismail & El-Sonbaty (2016). On the other hand, in the inflammation process, the release of pro-inflammatory cytokines as TNF-α, IL-1β, and IL-6 motivates NF-κB activation, as well as, the activated NF-κB trigger the release of the pro-inflammatory cytokines and mediates several signaling pathways (Han et al., 2006; Lestaevel et al., 2008; Eassawy et al., 2021). The results of the current study showed high levels of TNF-α, IL-1β, and IL-6 in the brain and liver tissues after exposure to gamma-radiation as reported previously (Ismail & El-Sonbaty, 2016; Eassawy et al., 2021; Yalcin et al., 2023). In addition, the activated pro-inflammatory cytokines and NF-κB cooperate to activate STAT3, which mediates the inflammation and apoptotic signals (Heinrich et al., 2003; Yoshida et al., 2004; Yuan et al., 2004; Grivennikov & Karin, 2010; Mohan et al., 2022). The data demonstrated up-regulation of NF-κB and STAT3 genes' expressions in the brain and liver tissues post exposure to gamma-radiation. Moreover, the caspase-3 level was boosted, as well as, the DNA fragmentation pattern revealed strand breaks/streaking of DNA in the brain and liver tissues of gamma-irradiated rats. DNA is the most susceptible molecule to gamma-irradiation destructive effects, due to the oxidative stress that cooperated with the developed inflammatory response, directing the cell to apoptosis.

However, the pretreatment of animals with FGE significantly minimized the activity of the hepatic marker enzymes (ALT, AST, ALP & GGT), TC, and TG levels of the γ-irradiated animals, which could be attributed to the potentiation of garlic bioactivity by yeast fermentation as described previously (Jung et al., 2011). Moreover, FGE ameliorated the SOD and GSH-Px activities in the cytosolic fraction of the brain and liver tissues, enhanced the GSH contents and declined MDA level in the brain and liver tissues in the rats exposed to a whole-body gamma-irradiation. The amelioration of SOD indicates the high detoxification effects of FGE on superoxide anion ($O_2^{\cdot -}$), hydroxyl radicals ($\cdot OH$), and hydrogen peroxide (H_2O_2). Moreover, the administration of FGE pre-exposure to γ-irradiation in rats has been shown to increase GSH content. Increasing the intracellular capacity for de novo synthesis of GSH-Px, which, uses GSH as a substrate, due to daily administration of FGE. Maintenance of the antioxidant enzymes activity and GSH contents

leads to a decrease of MDA towards the normal level in the brain and liver tissues of the irradiated animals. Since oxidative damage is implicated in the etiology of neurological complications, treatment with antioxidants has been used as a therapeutic approach in various types of neurodegenerative disease. The beneficial effects promoted by garlic could be attributed to the improvement of the antioxidant activity within the brain regions, and liver tissues, which potentially could result in reduction in the membrane lipids peroxidation (Rahman, 2003), consequently, a protection of brain and liver from free radicals is observed. Previous studies indicated that some of the chemical constituents of garlic can enhance the activities of detoxification glutathione enzymes (glutathione S-transferase, GSH-Px, and glutathione reductase) (Singh et al., 1995) and could suppress the formation of superoxide anion and hydrogen peroxide by improving the SOD, and catalase activities (Borek, 2001). Different protective pathways were evoked to explain the beneficial effects of garlic components. It includes: ROS scavenging, inhibition of LDL oxidation, protection of endothelial cell integrity by inhibition of LPO induced injury, inhibition of homocysteine thiolactone formation, enhancement of cellular GSH contents,, improving cellular scavenging enzymes, such as SOD, catalase, and GSH-Px, and inhibition of NF-κB (Saravanan & Prakash, 2004). Garlic is known to modulate LPO levels and enhance the antioxidant status (Arivazhagan et al., 2000). The beneficial effects of garlic can be attributed to the presence of organosulfur compounds (Balasenthil et al., 2000).

In addition, FGE extract pre-treatment showed anti-inflammatory effects in gamma-irradiated rats, whereas significant declines in the TNF-α, IL-1β and IL-6 levels, accompanied with down-regulation of NF-κB and STAT3 gene expression ratios in the brain and liver tissues of gamma-irradiated animals were observed. Regulation of the pro-inflammatory cytokine levels and NF-κB gene expression is involved in regulation of STAT3 gene expression, accordingly it can prevent apoptosis. Therefore, FGE extract pre-treatment regulated caspase-3 level and protect the DNA from gamma-irradiation damaging effects in the brain and liver tissues of gamma-irradiated animals. Moreover, the levels of Ca, Fe, Cu, Mg, Mn, and Zn were ameliorated in the cytosolic fractions of the brain and liver tissues of gamma-irradiated rats pretreated with FGE extract.

Garlic modulates LPO levels and enhances the antioxidant status (Balasenthil et al., 2000). Garlic extract ameliorated liver enzymes activity, ALT, AST (Shojaei-Zarghani et al., 2022), lipid profile; TG, TC, low and high density lipoprotein (Shabani et al., 2019), reduced the oxidative stress via reducing MDA level (Moosavian et al., 2020), and showed anti-inflammatory activity via reduction of TNF, and IL-6, levels (Darooghegi Mofrad et al., 2019), and suppressed NF-κB activation (Ban et al., 2009). Therefore, suppression of oxidative stress and the inflammatory response in irradiated rats by FGE leads to regulations of the trace elements levels in the brain and liver cytosolic fractions.

The beneficial effects of garlic can be attributed to the presence of organosulphur compounds (Balasenthil et al., 2000). Alliin (l-(+)-S-allylcystein sulfoxide) of garlic is transformed by alliinase enzyme into the active metabolite allicin, and diallyl sulfides (DAS). Allicin can boost the antioxidant status, scavenge ROS, and ameliorate GSH contents. S-Allyl Mercapto Cysteine (SAMC) is another garlic metabolite. DAS, and SAMC are hypolipidemic organosulfur compounds. The aqueous garlic extract is rich with S-Allylcysteine (SAC) that involved in the anti-inflammatory and antioxidant properties of garlic. SAC suppresses the inducible nitric oxide synthase (iNOs); reduced NO level, and regulate NF-κB and its signalling pathway. In addition, SAC demonstrated neuro-protective properties (Balasenthil et al., 2000; Yang et al., 2018; Li et al., 2023). The garlic constituent; diallyl trisulfide (DATS) suppressed NF-κB and STAT3 expressions in mice colon, via modulating their cysteine residue (Lee et al., 2013; Li et al., 2023). The garlic extract revealed anti-apoptotic activity via reduction of caspase 3 in rats' heart (Islam et al., 2020). An in-vitro study showed that garlic protects neurons against toxicity-induced apoptosis, mediated by inhibition of NF-κB (Peng et al., 2002). Pervious investigations confirmed that garlic extract demonstrated neuro-protective, and hepato-protective activities (Paolo & Pelini, 2022; Peng et al., 2002). The histopathological investigations demonstrate regulations of brain and liver morphological structures due to FGE pretreatment of gamma-irradiated rats. Fermentation with *S. cerevisiae* enhances the

sulfides' metabolites contents, as compared to the parent garlic extract (Paolo & Pelini, 2022). Therefore, garlic bioactivity is potentiated by yeast fermentation as described previously (Jung et al., 2011). Accordingly, FGE extract developed neuro-protective and hepato-protective activity on gamma-irradiation.

Conclusion

The results of the present study showed that *S. cerevisiae* FGE extract improved the in-vivo antioxidant system, demonstrated anti-inflammatory, and anti-apoptotic activities as well as protected the DNA that was isolated from the brain and liver tissues against fragmentation. These findings could suggest that the bioactivities of FGE showed neuro-hepato-protective effects on acute toxicity of whole-body gamma-irradiation mediated by regulation of the NF-κB and STAT3 signaling pathway in rats' brain and liver.

Acknowledgments: The authors are very thankful to the staff members of gamma-irradiation unit at the National Center of Radiation Research and Technology (NCRRT). Also, all authors would like to thank Dr. Sayed Abd E Raheem, Prof. of Pathology, Faculty of Medicine, Al-Azhar University, Cairo, Egypt, for his efforts to perform the histopathological examination.

References

Abd El-Haleem, M.R., Amer, M.G., Fares, A.E., Kamel, A.H.M. (2022) Evaluation of the Radioprotective Effect of Silver Nanoparticles on Irradiated Submandibular Gland of Adult Albino Rats. A Histological and Sialochemical Study. *BioNanoScience,* **12**(1), 13-27.

Akbarzadeh, T., Sabourian, R., Saeedi, M., Rezaeizadeh, H., Khanavi, M., Ardekani, M.R.S. (2015) Liver tonics: review of plants used in Iranian traditional medicine. *Asian Pacific Journal of Tropical Biomedicine,* **5**(3), 170-181.

Ansari, L., Banaei, A., Dastranj, L., Majdaeen, M., Vafapour, H., Zamani, H., et al. (2021) Evaluating the radioprotective effect of single dose and daily oral consumption of green tea, grape seed, and coffee bean extracts against gamma irradiation. *Applied Radiation and Isotopes: Including Data, Instrumentation and Methods for Use in Agriculture, Industry and Medicine,* **174**, 109781.

Ao, X., Yoo, J.S., Zhou, T.X., Wang, J.P., Meng, Q.W., Yan, L., et al. (2011) Effects of fermented garlic powder supplementation on growth performance, blood profiles and breast meat quality in broilers. *Livestock Science,* **141**(1), 85-89.

Arivazhagan, S., Balasenthil, S., Nagini, S. (2000) Garlic and neem leaf extracts enhance hepatic glutathione and glutathione dependent enzymes during N-methyl-N'-nitro-N-nitrosoguanidine (MNNG)-induced gastric carcinogenesis in rats. *Phytotherapy Research: PTR,* **14**(4), 291-293.

Balasenthil, S., Arivazhagan, S., Nagini, S. (2000) Garlic enhances circulatory antioxidants during 7, 12-dimethylbenz[a]anthracene-induced hamster buccal pouch carcinogenesis. *Journal of Ethnopharmacology,* **72**(3), 429-433.

Ban, J.O., Oh, J.H., Kim, T.M., Kim, D.J., Jeong, H.S., Han, S.B., Hong, J.T. (2009) Anti-inflammatory and arthritic effects of thiacremonone, a novel sulfur compound isolated from garlic via inhibition of NF-kappaB. *Arthritis Research & Therapy,* **11**(5), R145. DOI: 10.1186/ar2819.

Bancroft, J.D., Layton, C. (2019) The hematoxylins and eosin (Ch. 10), In: "*Theory and Practice of Histological Techniques*", Kim Suvarna S., Layton C., and Bancroft, J.D. (Eds.), 8th ed., pp 126–138. Churchill Livingstone, Edinburgh, London, Melbourne and New York.

Borek, C. (2001) Antioxidant health effects of aged garlic extract. *Journal of Nutrition,* **131**(3s), 1010s-1015s.

Chae, J., Lee, E., Oh, S.M., Ryu, H.W., Kim, S., Nam, J.O. (2023) Aged black garlic (*Allium sativum* L.) and aged black elephant garlic (*Allium ampeloprasum* L.) alleviate obesity and attenuate obesity-induced muscle atrophy in diet-induced obese C57BL/6 mice. *Biomedicine & Pharmacotherapy= Biomedecine & pharmacotherapie,* **163**, 114810. DOI: 10.1016/j.biopha.2023.114810.

Darooghegi Mofrad, M., Milajerdi, A., Koohdani, F., Surkan, P.J., Azadbakht, L. (2019) Garlic Supplementation Reduces Circulating C-reactive Protein, Tumor Necrosis Factor, and Interleukin-6 in Adults: A Systematic Review and Meta-analysis of Randomized Controlled Trials. *Journal of Nutrition,* **149**(4), 605-618.

Díaz-Muñoz, C., Verce, M., De Vuyst, L., Weckx, S. (2022) Phylogenomics of a Saccharomyces cerevisiae cocoa strain reveals adaptation to a West African fermented food population. *iScience,* **25**(11), 105309. DOI: https://doi.org/10.1016/j.isci.2022.105309.

Ding, H., Ao, C., Zhang, X. (2023) Potential use of garlic products in ruminant feeding: A review. *Animal Nutrition (Zhongguo xu mu shou yi xue hui),* **14**, 343-355.

Eassawy, M.M.T., Salem, A.A., Ismail, A.F.M. (2021) Biochemical study on the protective effect of curcumin on acetaminophen and gamma-irradiation induced hepatic toxicity in rats. *Environmental Toxicology,* **36**, 748–763.

Ellman, G.L. (1959) Tissue sulfhydryl groups. *Archives of Biochemistry and Biophysics,* **82**(1), 70-77.

El-Saber Batiha, G., Beshbishy, A.M., Wasef, L.G., Elewa, Y.H.A., Al-Sagan, A.A., et al. (2020) Chemical Constituents and Pharmacological Activities of Garlic (*Allium sativum* L.): A Review. *Nutrients,* **12**(3). DOI: 10.3390/nu12030872.

Feurgard, C., Bayle, D., Guézingar, F., Sérougne, C., Mazur, A., Lutton, C., Aigueperse, J., Gourmelon, P., Mathé, D. (1998) Effects of ionizing radiation (neutrons/gamma rays) on plasma lipids and lipoproteins in rats. *Radiation Research,* **150**(1), 43-51.

Frankenberg-Schwager, M., Frankenberg, D. (1990) DNA double-strand breaks: their repair and relationship to cell killing in yeast. *International Journal of Radiation Biology,* **58**(4), 569-575.

Grivennikov, S.I., Karin, M. (2010) Dangerous liaisons: STAT3 and NF-kappaB collaboration and crosstalk in cancer. *Cytokine & Growth Factor Reviews,* **21**(1), 11-19.

Halliwell, B., Aruoma, O.I. (1991) DNA damage by oxygen-derived species. Its mechanism and measurement in mammalian systems. *FEBS Letters,* **281**(1-2), 9-19.

Han, S.K., Song, J.Y., Yun, Y.S., Yi, S.Y. (2006) Effect of gamma radiation on cytokine expression and cytokine-receptor mediated STAT activation. *International Journal of Radiation Biology,* **82**(9), 686-697.

Heinrich, P.C., Behrmann, I., Haan, S., Hermanns, H.M., Müller-Newen, G., Schaper, F. (2003) Principles of interleukin (IL)-6-type cytokine signalling and its regulation. *The Biochemical Journal,* **374**(Pt 1), 1-20.

Herrera-Calderon, O., Chacaltana-Ramos, L.J., Huayanca-Gutiérrez, I.C., Algarni, M.A., Alqarni, M., Batiha, G.E. (2021) Chemical constituents, *in vitro* antioxidant activity and *in silico* study on NADPH oxidase of *Allium sativum* L. (garlic) essential oil. *Antioxidants (Basel, Switzerland),* **10**(11). DOI: 10.3390/antiox10111844.

Hussien, S.M. (2023) The impact of cyclophosphamide versus high-level of ionizing radiation on the immune response. *Heliyon,* **9**(7), e18025. DOI: 10.1016/j.heliyon.2023.e18025.

Ibrahim, N., Eldahshan, O.A., Elshawi, O.E. (2023) Phytochemical screening and radioprotective potential of Jasminum grandiflorum methanol extract against gamma irradiation-induced oxidative damage and diverse inflammatory mediators in lungs of male Swiss Albino Rats. *Natural Product Research*. DOI: https://doi.org/10.1080/14786419.2023.2181801.

Ide, N., Lau, B.H.S. (2001) Garlic compounds minimize intracellular oxidative stress and inhibit nuclear Factor-κB activation. *The Journal of Nutrition,* **131**(3), 1020S-1026S.

Islam, D., Banerjee Shanta, M., Akhter, S., Lyzu, C., Hakim, M., Islam, M.R., Mohanta, L.C., Lipy, E.P., Roy, D.C. (2020) Cardioprotective effect of garlic extract in isoproterenol-induced myocardial infarction in a rat model: assessment of pro-apoptotic caspase-3 gene expression. *Clinical Phytoscience,* **6**(1), 67. DOI: 10.1186/s40816-020-00199-4.

Ismail, A.F., El-Sonbaty, S.M. (2016) Fermentation enhances Ginkgo biloba protective role on gamma-irradiation induced neuroinflammatory gene expression and stress hormones in rat brain. *Journal of Photochemistry and Photobiology B, Biology,* **158**, 154-163.

Ismail, A.F., Salem, A.A., Eassawy, M.M. (2016a) Modulation of gamma-irradiation and carbon tetrachloride induced oxidative stress in the brain of female rats by flaxseed oil. *Journal of Photochemistry and Photobiology B, Biology,* **161**, 91-99.

Ismail, A.F.M., Salem, A.A.M., Eassawy, M.M.T. (2016b) Hepatoprotective effect of grape seed oil against carbon tetrachloride induced oxidative stress in liver of γ-irradiated rat. *Journal of Photochemistry and Photobiology B: Biology,* **160**, 1-10. DOI:

Jeong, Y.Y., Ryu, J.H., Shin, J.H., Kang, M.J., Kang, J.R., Han, J., Kang, D. (2016) Comparison of anti-oxidant and anti-inflammatory effects between fresh and aged black garlic extracts. *Molecules (Basel, Switzerland),* **21**(4), 430. DOI: 10.3390/molecules21040430.

Jung, Y.M., Lee, S.H., Lee, D.S., You, M.J., Chung, I.K., Cheon, W.H., et al. (2011) Fermented garlic protects diabetic, obese mice when fed a high-fat diet by antioxidant effects. *Nutrition Research (New York, NY),* **31**(5), 387-396.

Kim, S.H., Jung, E.Y., Kang, D.H., Chang, U.J., Hong, Y.H., Suh, H.J. (2012) Physical stability, antioxidative properties, and photoprotective effects of a functionalized formulation containing black garlic extract. *Journal of Photochemistry and Photobiology B, Biology,* **117**, 104-110.

Lee, Y.M., Gweon, O.C., Seo, Y.J., Im, J., Kang, M.J., Kim, M.J., Kim, J.I. (2009) Antioxidant effect of garlic and aged black garlic in animal model of type 2 diabetes mellitus. *Nutrition Research and Practice,* **3**(2), 156-161.

Lee, H.J., Lee, H.G., Choi, K.S., Surh, Y.J., Na, H.K. (2013) Diallyl trisulfide suppresses dextran sodium sulfate-induced mouse colitis: NF-κB and STAT3 as potential targets. *Biochem Biophys Res Commun,* **437**(2), 267-273. .

Lee, Y.H., Ahmadi, F., Kim, Y.I., Oh, Y.K., Kwak, W.S. (2020) Co-ensiling garlic stalk with citrus pulp improves the fermentation quality and feed-nutritional value. *Asian-Australasian Journal of Animal Sciences,* **33**(3), 436-445.

Lestaevel, P., Grandcolas, L., Paquet, F., Voisin, P., Aigueperse, J., Gourmelon, P. (2008) Neuro-inflammatory response in rats chronically exposed to 137Cesium. *Neurotoxicology,* **29**(2), 343-348.

Li, B., Li, J., Akbari, A., Baziyar, P., Hu, S. (2023) Evaluation of Expression of Cytochrome P450 Aromatase and Inflammatory, Oxidative, and Apoptotic Markers in Testicular Tissue of Obese Rats (Pre)Treated with Garlic Powder. *Evidence-based Complementary and Alternative Medicine : eCAM,* **2023**, 4858274. DOI: 10.1155/2023/4858274.

Liu, K.X., He, W., Rinne, T., Liu, Y., Zhao, M.Q., Wu, W.K. (2007) The effect of ginkgo biloba extract (EGb 761) pretreatment on intestinal epithelial apoptosis induced by intestinal ischemia/reperfusion in rats: role of ceramide. *The American Journal of Chinese Medicine,* **35**(5), 805-819.

Livak, K.J., Schmittgen, T.D. (2001) Analysis of relative gene expression data using real-time quantitative PCR and the 2(-Delta Delta C(T)) Method. *Methods (San Diego, Calif),* **25**(4), 402-408.

Lowry, O.H., Rosebrough, N.J., Farr, A.L., Randall, R.J. (1951) Protein measurement with the folin phenol reagent. *Journal of Biological Chemistry,* **193**(1), 265–275.

Minami, M., Yoshikawa, H. (1979) A simplified assay method of superoxide dismutase activity for clinical use. *Clinica Chimica Acta; International Journal of Clinical Chemistry,* **92**(3), 337-342.

Mohan, C.D., Rangappa, S., Preetham, H.D., Chandra Nayaka, S., Gupta, V.K., Basappa, S., et al. (2022) Targeting STAT3 signaling pathway in cancer by agents derived from Mother Nature. *Seminars in Cancer Biology,* **80**, 157-182.

Mondal, A., Banerjee, S., Bose, S., Mazumder, S., Haber, R.A., Farzaei, M.H., Bishayee, A. (2022) Garlic constituents for cancer prevention and therapy: From phytochemistry to novel formulations. *Pharmacological Research,* **175**, 105837. DOI: 10.1016/j.phrs.2021.105837.

Moosavian, S.P., Arab, A., Paknahad, Z., Moradi, S. (2020) The effects of garlic supplementation on oxidative stress markers: A systematic review and meta-analysis of randomized controlled trials. *Complementary Therapies in Medicine,* **50**, 102385. DOI: 10.1016/j.ctim.2020.102385.

Moslehi-Jenabian, S., Pedersen, L.L., Jespersen, L. (2010) Beneficial effects of probiotic and food borne yeasts on human health. *Nutrients,* **2**(4), 449-473.

Okamura, T., Miura, T., Takemura, G., Fujiwara, H., Iwamoto, H., Kawamura, S., et al. (2000) Effect of caspase inhibitors on myocardial infarct size

and myocyte DNA fragmentation in the ischemia-reperfused rat heart. *Cardiovascular Research,* **45**(3), 642-650.

Owis, A.I., Sherif, N.H., Hassan, A.A., El-Naggar, E.-M.B., El-Khashab, I.H., El-Ghaly, E.-S. (2023) *Tropaeolum majus* L. and low dose gamma radiation suppress liver carcinoma development via EGFR-HER2 signaling pathway. *Natural Product Research,* **37**(6), 1030-1035.

Ozmen, O., Kavrik, O. (2020) Ameliorative effects of vitamin C against hepatic pathology related to Wi-Fi (2.45 GHz electromagnetic radiation) in rats. *Iranian Journal of Radiation Research,* **18**, 405-412.

Paolo, P., Pelini, P. (2022) Action of *Saccharomyces cerevisiae* yeast in the production and metabolic activity of black garlic. *Zenodo*. https://doi.org/10.5281/zenodo.6614657.

Peng, Q., Buz'Zard, A.R., Lau, B.H. (2002) Neuroprotective effect of garlic compounds in amyloid-beta peptide-induced apoptosis *in vitro. Medical Science Monitor: International Medical Journal of Experimental and Clinical Research,* **8**(8), Br328-337.

Pineton de Chambrun, G., Neut, C., Chau, A., Cazaubiel, M., Pelerin, F., Justen, P., Desreumaux, P. (2015) A randomized clinical trial of Saccharomyces cerevisiae versus placebo in the irritable bowel syndrome. *Digestive and Liver Disease,* **47**(2), 119-124.

Poloni, V., Magnoli, A., Fochesato, A., Cristofolini, A., Caverzan, M., Merkis, C., et al. (2020) A Saccharomyces cerevisiae RC016-based feed additive reduces liver toxicity, residual aflatoxin B1 levels and positively influences intestinal morphology in broiler chickens fed chronic aflatoxin B1-contaminated diets. *Animal Nutrition (Zhongguo xu mu shou yi xue hui),* **6**(1), 31-38.

Queiroz, Y.S.d., Ishimoto, E.Y., Bastos, D.H.M., Sampaio, G.R., Torres, E.A.F.d.S. (2009) Garlic (*Allium sativum* L.) and ready-to-eat garlic products: In vitro antioxidant activity. *Food Chemistry,* **115**, 371-374.

Rageh, M.M., El-Gebaly, R.H. (2018) Melanin nanoparticles: Antioxidant activities and effects on γ-ray-induced DNA damage in the mouse. *Mutation Research/Genetic Toxicology and Environmental Mutagenesis,* **828**, 15-22.

Rahman, K. (2003) Garlic and aging: new insights into an old remedy. *Ageing Research Reviews,* **2**(1), 39-56.

Rotruck, J.T., Pope, A.L., Ganther, H.E., Swanson, A.B., Hafeman, D.G., Hoekstra, W.G. (1973) Selenium: Biochemical role as a component of glutathione peroxidase. *Science (New York, NY),* **179**(4073), 588-590.

Rouf, R., Uddin, S.J., Sarker, D.K., Islam, M.T., Ali, E.S., Shilpi, J.A., et al. (2020) Antiviral potential of garlic (*Allium sativum*) and its organosulfur compounds: A systematic update of pre-clinical and clinical data. *Trends in Food Science & Technology,* **104**, 219-234.

Sahoo, G., Samal, D., Khandayataray, P., Murthy, M.K. (2023) A Review on Caspases: Key Regulators of Biological Activities and Apoptosis. *Molecular Neurobiology,* **60**(10), 5805-5837.

Salem, A.M., Mohammaden, T.F., Ali, M.A.M., Mohamed, E.A., Hasan, H.F. (2016) Ellagic and ferulic acids alleviate gamma radiation and aluminium chloride-induced oxidative damage. *Life Sciences,* **160**, 2-11.

Santos, N., Silva, R.F., Pinto, M., Silva, E.B.D., Tasat, D.R., Amaral, A. (2017) Active caspase-3 expression levels as bioindicator of individual radiosensitivity. *Anais da Academia Brasileira de Ciencias,* **89**(1 Suppl 0), 649-659.

Saravanan, G., Prakash, J. (2004) Effect of garlic (*Allium sativum*) on lipid peroxidation in experimental myocardial infarction in rats. *Journal of Ethnopharmacology,* **94**(1), 155-158.

Satoh, K. (1978) Serum lipid peroxide in cerebrovascular disorders determined by a new colorimetric method. *Clinica Chimica Acta; International Journal of Clinical Chemistry,* **90**(1), 37-43.

Savairam, V.D., Patil, N.A., Borate, S.R., Ghaisas, M.M., Shete, R.V. (2023) Allicin: A review of its important pharmacological activities. *Pharmacological Research- Modern Chinese Medicine*, **8**, 100283. 13 pages. https://doi.org/10.1016/j.prmcm.2023.100283.

Shabani, E., Sayemiri, K., Mohammadpour, M. (2019) The effect of garlic on lipid profile and glucose

parameters in diabetic patients: A systematic review and meta-analysis. *Primary Care Diabetes,* **13**(1), 28-42.

Shojaei-Zarghani, S., Fattahi, M.R., Kazemi, A., Safarpour, A.R. (2022) Effects of garlic and its major bioactive components on non-alcoholic fatty liver disease: A systematic review and meta-analysis of animal studies. *Journal of Functional Foods,* **96**, 105206. DOI: https://doi.org/10.1016/j.jff.2022.105206.

Singh, S.P., Abraham, S.K., Kesavan, P.C. (1995) In vivo radioprotection with garlic extract. *Mutation Research/Genetic Toxicology,* **345**(3), 147-153.

Timmons, M.D., Bradley, M.A., Lovell, M.A., Lynn, B.C. (2011) Procedure for the isolation of mitochondria, cytosolic and nuclear material from a single piece of neurological tissue for high-throughput mass spectral analysis. *Journal of Neuroscience Methods,* **197**(2), 279-282.

Uzun, S.G., Altunkaynak, B.Z., Alkan, I. (2023) The effects of myricitrin and chebulinic acid on the rat hippocampus exposed to gamma radiation: A stereological, histochemical and biochemical study. *Journal of Chemical Neuroanatomy,* **132**, 102305. DOI: 10.1016/j.jchemneu.2023.102305.

Varela, C., Alperstein, L., Sundstrom, J., Solomon, M., Brady, M., Borneman, A., Jiranek, V. (2023) A special drop: Characterising yeast isolates associated with fermented beverages produced by Australia's indigenous peoples. *Food Microbiology,* **112**, 104216.

Wallace, S.S. (1998) Enzymatic processing of radiation-induced free radical damage in DNA. *Radiation research,* **150**(5 Suppl), S60-79.

Wang, S.W., Ren, B.X., Qian, F., Luo, X.Z., Tang, X., Peng, X.C., et al. (2019) Radioprotective effect of epimedium on neurogenesis and cognition after acute radiation exposure. *Neuroscience Research,* **145**, 46-53.

Ward, J.F. (1999) Ionizing Radiation Damage to DNA. In: "*Advances in DNA Damage and Repair: Oxygen Radical Effects, Cellular Protection, and Biological Consequences*", M. Dizdaroglu, and A.E. Karakaya (Eds.), pp. 431-439, Boston, MA: Springer US.

Wei, J., Wang, B., Wang, H., Meng, L., Zhao, Q., Li, X., et al. (2019) Radiation-induced normal tissue damage: oxidative stress and epigenetic mechanisms. *Oxidative Medicine and Cellular Longevity,* **2019**, 3010342. DOI: 10.1155/2019/3010342.

Yalcin, B., Yay, A.H., Tan, F.C., Özdamar, S., Yildiz, O.G. (2023) Investigation of the anti-oxidative and anti-inflammatory effects of melatonin on experimental liver damage by radiation. *Pathology, Research and Practice,* **246**, 154477. DOI: 10.1016/j.prp.2023.154477.

Yang, C., Li, L., Yang, L., Lǔ, H., Wang, S., Sun, G. (2018) Anti-obesity and hypolipidemic effects of garlic oil and onion oil in rats fed a high-fat diet. *Nutrition & Metabolism,* **15**, 43. DOI: 10.1186/s12986-018-0275-x.

Yoshida, Y., Kumar, A., Koyama, Y., Peng, H., Arman, A., Boch, J.A., Auron, P.E. (2004) Interleukin 1 activates STAT3/nuclear factor-kappaB cross-talk via a unique TRAF6- and p65-dependent mechanism. *The Journal of Biological Chemistry,* **279**(3), 1768-1776.

Yuan, Z.L., Guan, Y.J., Wang, L., Wei, W., Kane, A.B., Chin, Y.E. (2004) Central role of the threonine residue within the p+1 loop of receptor tyrosine kinase in STAT3 constitutive phosphorylation in metastatic cancer cells. *Molecular and Cellular Biology,* **24**(21), 9390-9400.

Zaher, N.H., Salem, A.A., Ismail, A.F. (2016) Novel amino acid derivatives bearing thieno[2,3-d] pyrimidine moiety down regulate NF-κB in γ-irradiation mediated rat liver injury. *Journal of Photochemistry and Photobiology B, Biology,* **165**, 328-339.